Journal of Power Sources 188 (2009) 564–569

Contents lists available at ScienceDirect

Journal of Power Sources

journal homepage: www.elsevier.com/locate/jpowsour

Cycle life improvement of ZrO_2-coated spherical $LiNi_{1/3}Co_{1/3}Mn_{1/3}O_2$ cathode material for lithium ion batteries

Shao-Kang Hu[a], Geng-Hao Cheng[a], Ming-Yao Cheng[a], Bing-Joe Hwang[a,b,*], Raman Santhanam[a,1]

[a] Nanoelectrochemistry Laboratory, Department of Chemical Engineering, National Taiwan University of Science and Technology, Taipei 106, Taiwan
[b] National Synchrotron Radiation Research Center, Hsinchu 300, Taiwan

ARTICLE INFO

Article history:
Received 23 May 2008
Received in revised form
27 November 2008
Accepted 28 November 2008
Available online 3 December 2008

Keywords:
Spherical $LiNi_{1/3}Co_{1/3}Mn_{1/3}O_2$
ZrO_2 coating
Cycling performance
Lithium battery

ABSTRACT

A modified synthesis process was developed based on co-precipitation method followed by spray drying process. In this process, a spherical shaped $(Co_{1/3}Ni_{1/3}Mn_{1/3})(OH)_2$ precursor was synthesized by co-precipitation and pre-heated at 500 °C to form a high structural stability spinel $(CoNiMn)O_4$ to maintain its shape for further processing. The spherical $LiNi_{1/3}Co_{1/3}Mn_{1/3}O_2$ was then prepared by spray drying process using spherical spinel $(CoNiMn)O_4$. $LiNi_{1/3}Co_{1/3}Mn_{1/3}O_2$ powders were then modified by coating their surface with a uniform and nano-sized layer of ZrO_2. The ZrO_2-coated $LiNi_{1/3}Co_{1/3}Mn_{1/3}O_2$ material exhibited an improved rate capability and cycling stability under a high cut-off voltage of 4.5 V. X-ray diffraction (XRD) measurements revealed that the material had a well-ordered layered structure and Zr was not doped into the $LiNi_{1/3}Co_{1/3}Mn_{1/3}O_2$. Electrochemical impedance spectroscopy measurements showed that the coated material has stable cell resistance regardless of cycle number. The interrupt charging/discharging test indicated that the ZrO_2 coating can suppress the polarization effects during the charging and discharging process. From these results, it is believed that the improved cycling performance of ZrO_2-coated $LiNi_{1/3}Co_{1/3}Mn_{1/3}O_2$ is attributed to the ability of ZrO_2 layer in preventing direct contact of the active material with the electrolyte resulting in a decrease of electrolyte decomposition reactions.

1. Introduction

Lithium ion batteries have become the state-of-the-art power sources for portable appliances such as notebook computers, cellular phones, and digital cameras and also a prime candidate for hybrid electric vehicles (HEVs), plug-in hybrid electric vehicles (PHEVs) and electric vehicles (EVs) for reasons of high energy density, high power density, better cyclability and safety [1–3]. Lithium transition metal oxides and their derivatives, such as $LiCoO_2$, $LiMn_2O_4$, $LiNiCoO_2$, $LiNi_{1-x}Co_xO_2$ and so on have been studied extensively and they are available commercially as 4 V class cathode materials for lithium ion batteries. Among them, $LiCoO_2$ has been used as a major cathode material for lithium ion batteries since Sony Corporation firstly introduced lithium ion batteries containing carbon anode and a $LiCoO_2$ cathode separated by non-aqueous electrolyte in 1990. Obviously, it is an excellent cathode material with low irreversible capacity loss and good cycling performance. The practical capacity of lithium ion battery has been increased gradually by intensive research for both cathode and anode materials. The relatively high cost, concerns about the thermal stability of the charged cathode material in electrolyte, and the lure of larger specific capacity has stimulated the study of possible cathode materials for lithium ion batteries.

Extensive studies have been carried out to improve the performance of the cathode active materials by cationic substitution. Recently, manganese based layered compounds as cathode materials for lithium ion batteries are of great interest and are potential candidates to replace the commercial $LiCoO_2$. These include $LiNi_{1/2}Mn_{1/2}O_2$ [4,5], $LiNi_{1/3}Co_{1/3}Mn_{1/3}O_2$ [6–10], and its derivatives such as $LiNi_xCo_{1-2x}Mn_xO_2$ ($0 \leqq x \leqq 1/3$) [11–13]. The electrochemical processes involve the redox pair of Ni^{2+}/Ni^{4+} with two-electron transfer in the series of these compounds [5,9,11]. Among them, $LiNi_{1/3}Co_{1/3}Mn_{1/3}O_2$ has been studied extensively as promising cathode material for lithium ion batteries. The layered $LiNi_{1/3}Co_{1/3}Mn_{1/3}O_2$ has drawn much attention as it exhibits much higher capacity of closer to 200 mA h g^{-1} with enhanced safety [14–18]. Electronic structure studies have shown that it consists of Ni^{2+}, Mn^{4+} and Co^{3+}, and reversible capacity involves the oxidation of Ni^{2+} to Ni^{4+} with a two-electron transfer during the initial stage of Co^{3+} to Co^{4+} in the later stage [19–21]. Thus the higher capacity of layered $LiNi_{1/3}Co_{1/3}Mn_{1/3}O_2$ could be due to the improved chemical stability associated $Ni^{2+/3+}$ and the $Ni^{3+/4+}$ redox couple compared to $Co^{3+/4+}$ redox couple. However, it has been reported that the poor

* Corresponding author at: Nanoelectrochemistry Laboratory, Department of Chemical Engineering, National Taiwan University of Science and Technology, Taipei 106, Taiwan. Tel.: +886 2 27376624; fax: +886 2 27376644.
E-mail address: bjh@mail.ntust.edu.tw (B.-J. Hwang).
[1] Present address: Nanoexa Corporation, Burlingame, CA, USA.

0378-7753/$ – see front matter © 2008 Published by Elsevier B.V.
doi:10.1016/j.jpowsour.2008.11.113

electrochemical properties of layered $LiNi_{1/3}Co_{1/3}Mn_{1/3}O_2$ at high voltage are due to the polarization effect and the electrolyte decomposition [22]. Moreover, even at upper voltage limits of 4.4–4.5 V, capacity fading was still observed upon cycling. The origin of this capacity fading was mainly attributed to gradual decaying of electroactive Co as reported by Shaju et al. [23].

An alternate approach to improve electrochemical performance is to change the surface properties of the cathode material by coating its particle with some metal oxides to avoid the unwanted reactions on the surface and protect the bulk. Recently, Chen and Dahn reported that the cycle-life performance of $LiCoO_2$ was improved by a ZrO_2 coating [24]. Similarly, other groups reported that a metal oxide coating by a sol–gel method significantly improved the electrochemical properties of $LiCoO_2$ without significantly specific capacity loss, and that the metal oxide coating layer acted as solid electrolyte with a reasonable high Li ion conductivity [25–30].

In this article, we show that the developed synthesis process is able to synthesize spherical $LiNi_{1/3}Co_{1/3}Mn_{1/3}O_2$ active material and also to coat a uniform ZrO_2 layer on the synthesized active material. We study the effect of surface modification of the $LiNi_{1/3}Co_{1/3}Mn_{1/3}O_2$ by ZrO_2 coating on the electrochemical performance at high-voltage region. We also investigate the possible reasons for enhanced electrochemical performance by comparing structural stability and impedance variation during cycling process of pristine and ZrO_2-coated spherical $LiNi_{1/3}Co_{1/3}Mn_{1/3}O_2$.

2. Experimental

The Ni–Co–Mn mixed hydroxide powders were prepared by co-precipitation method. An aqueous solution of lithium hydroxide ($LiOH{\cdot}H_2O$), nickel nitrate ($Ni(NO_3)_2{\cdot}6H_2O$), cobalt nitrate ($Co(NO_3)_2{\cdot}6H_2O$) and manganese nitrate ($Mn(NO_3)_2{\cdot}4H_2O$) was stirred continuously at room temperature. Simultaneously, an appropriate amount of LiOH solution and the required amount of NH_4OH solution as a chelating agent were added to the above solution continuously. The co-precipitated hydroxide powder $(Co_{1/3}Ni_{1/3}Mn_{1/3})(OH)_2$ was pre-heated at 500 °C for 5 h in air to form a spinel $CoNiMnO_4$. To synthesize $LiNi_{1/3}Co_{1/3}Mn_{1/3}O_2$ material, a stoichiometric amount of $CoNiMnO_4$ powder and LiOH was dispersed in ethanol solution to form a well-mixed $CoNiMnO_4$/LiOH precursor. The resulting precursor solution was dried to form a mixed dry precursor via a spray-dryer. The as-prepared precursor powders were ground and sintered at 450 °C for 6 h and then at 900 °C for 12 h to form $LiNi_{1/3}Co_{1/3}Mn_{1/3}O_2$ material. The heating and cooling rate of the heat treatment was 2 °C/min. The ZrO_2-modified $LiNi_{1/3}Co_{1/3}Mn_{1/3}O_2$ was prepared by mixing the spherical $LiNi_{1/3}Co_{1/3}Mn_{1/3}O_2$ and $Zr(OC_3H_7)_4$ in 1-propanol. The entire process was carried out under continuous stirring at room temperature. The prepared solution was heated in a beaker in a temperature range of 80–90 °C until a transparent sol was obtained. The resulting precursor was sintered at 450 °C for 5 h to obtain the surface-modified spherical $LiNi_{1/3}Co_{1/3}Mn_{1/3}O_2$.

The Li, Co, Ni and Mn contents in the resulting materials were analyzed using an inductively coupled plasma/atomic emission spectrometer (ICP/AES, Kontron S-35). The phase purity was verified from powder X-ray diffraction measurements (XRD, Rigaku D/max-b) using Cu K_α radiation. The particle morphology of the powders after calcination was obtained using a scanning electron microscopy (SEM, Hitachi S-4100). Electrochemical characterization was carried out with a coin-type cell. The synthesized $LiNi_{1/3}Co_{1/3}Mn_{1/3}O_2$ cathode was prepared by mixing an 85:3.5:1.5:10 (w/w) ratio of active materials, carbon black, KS6 graphite and polyvinylidene fluoride binder, respectively, in N-methyl pyrrolidinone. The resulting paste was cast on an aluminum current collector. The entire assembly was dried under vacuum overnight and then heated in an oven at 120 °C for 2 h. Lithium metal (FMC) was used as an anode and a polypropylene separator was used to separate the anode and the cathode. 1.0 M $LiPF_6$ dissolved in a 1:1 mixture of ethylene carbonate (EC)/diethyl carbonate (DEC) was used as an electrolyte. The cells were assembled in an argon-filled dry box where both the moisture and oxygen contents were less than 1 ppm.

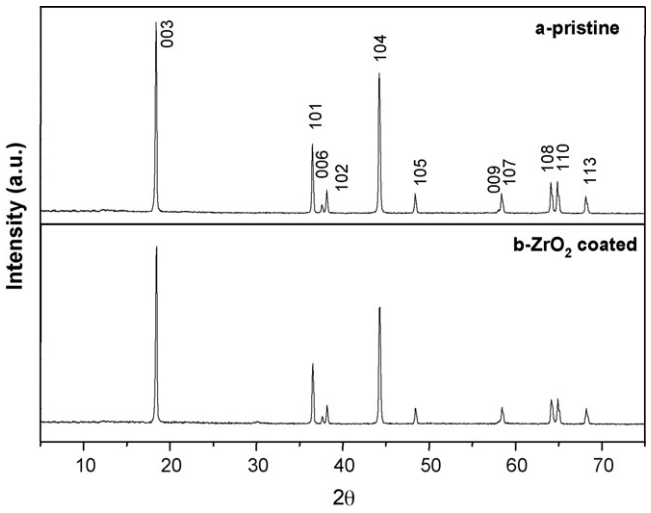

Fig. 1. XRD patterns of spherical (a) $LiNi_{1/3}Co_{1/3}Mn_{1/3}O_2$ and (b) ZrO_2-coated $LiNi_{1/3}Co_{1/3}Mn_{1/3}O_2$.

3. Results and discussion

The XRD patterns of the spherical $LiNi_{1/3}Co_{1/3}Mn_{1/3}O_2$ and ZrO_2-coated $LiNi_{1/3}Co_{1/3}Mn_{1/3}O_2$ are presented in Fig. 1a and b, respectively. All the diffraction peaks can be indexed as a layered oxide structure based on a hexagonal α-$NaFeO_2$ structure (space group $R\bar{3}m$). No impurities and secondary phases are observed in this figure. The structure has Li ions at the 3a, the transition metal ions (M = Co, Ni, Mn) at 3b and O ions at 6c sites. Due to the similarity of the ionic radii of Ni^{2+} (0.69 Å) and Li^+ (0.76 Å), a partial interchange of occupancy of Li and nickel ions among the sites (i.e. Li in 3b and Ni in 3a sites) are expected and that would give rise to disordering in the structure called 'cation mixing' [24]. It has been established that cation mixing is known to deteriorate the electrochemical performance of the above-layered compounds. The integrated intensity ratio of the (0 0 3) to (1 0 4) lines (R) in the XRD patterns was shown to be a measurement of the cation mixing and a value of $R < 1.2$ is an indication of undesirable cation mixing [24]. The oxygen sublattice in the α-$NaFeO_2$ type structure is considered as distorted from the fcc array in the direction of hexagonal c-axis [25,26]. This distortion gives rise to a splitting of the lines assigned to the Miller indices (0 0 6, 1 0 2) and (1 0 8, 1 1 0) in the XRD patterns and these are characteristic to the layer structure. The lattice parameters of spherical $LiNi_{1/3}Co_{1/3}Mn_{1/3}O_2$ and ZrO_2-coated $LiNi_{1/3}Co_{1/3}Mn_{1/3}O_2$ materials were calculated by the Rietveld refinement and the results were summarized in Table 1. It is clear that there is no significant difference in the crystal struc-

Table 1
Structural parameters of spherical $LiNi_{1/3}Co_{1/3}Mn_{1/3}O_2$ and ZrO_2-coated $LiNi_{1/3}Co_{1/3}Mn_{1/3}O_2$.

Materials	a (Å)	c (Å)	c/a	$I_{(003)}/I_{(104)}$	Grain size (nm)
$LiNi_{1/3}Co_{1/3}Mn_{1/3}O_2$	2.882	14.38	4.99	1.367	54.7
ZrO_2-coated $LiNi_{1/3}Co_{1/3}Mn_{1/3}O_2$	2.875	14.32	4.98	1.365	56.8

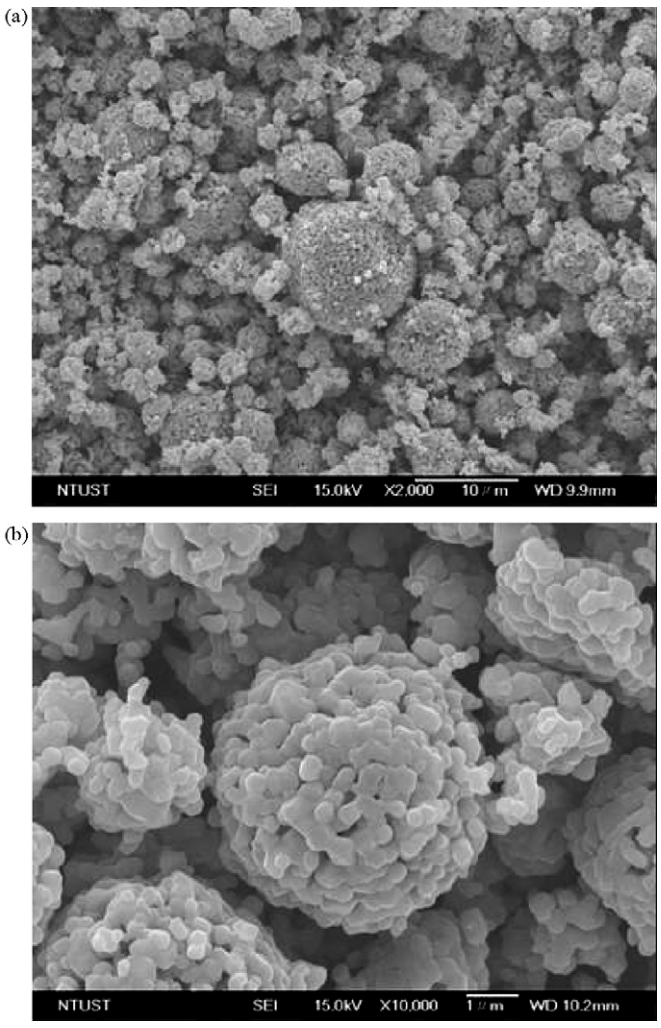

Fig. 2. SEM images of spherical $LiNi_{1/3}Co_{1/3}Mn_{1/3}O_2$ at different magnifications: (a) 2000× and (b) 10,000×.

ture of $LiNi_{1/3}Co_{1/3}Mn_{1/3}O_2$ after coated with ZrO_2 as can be seen in Fig. 1 and Table 1. This result suggests that Zr is not doped in the $LiNi_{1/3}Co_{1/3}Mn_{1/3}O_2$ because the coated amount is very small and the coating thickness is less than 25 nm. This is confirmed by TEM measurements and will be shown later in this work. In fact, the lattice parameter "*a*" is related to average metal–oxygen distance and if this distance is changed significantly, it clearly indicates that foreign ions should be doped into the crystal structure of parent material. Hence, in this work, it is believed that ZrO_2 is coated only on the surface of $LiNi_{1/3}Co_{1/3}Mn_{1/3}O_2$ as a very thin layer. Clear splitting of (0 0 6)/(1 0 2) and (1 0 8)/(1 1 0) peak pairs in the XRD pattern and the *c*/*a* ratio (4.99 and 4.98) well above that required for distortion of oxygen lattice which reveal that the layered structure is formed [26]. The ratio of the intensities of the (0 0 3) and (1 0 4) peaks are 1.367 and 1.365, well above the values reported for compounds like $LiNi_{1-x}Co_xO_2$ and $LiNiO_2$ to deliver good electrochemical performance [23,26].

In order to observe morphology of the spherical $LiNi_{1/3}Co_{1/3}Mn_{1/3}O_2$ and ZrO_2-modified spherical $LiNi_{1/3}Co_{1/3}Mn_{1/3}O_2$ materials, SEM and TEM measurements were carried out at different magnifications. Scanning electron micrographs of pristine and coated materials were given in Fig. 2. Fig. 2a and b shows the micro morphologies of spherical $LiNi_{1/3}Co_{1/3}Mn_{1/3}O_2$ materials in various magnifications, respectively. Generally, excellent rate capability can be achieved from particles with small particle (high surface area) size but the tap density would be low. High tap density is one of the important requirements for the cathode materials because it influences the volumetric capacity of the commercial lithium ion batteries. However, as can be seen in Fig. 2a, the primary particle size is about 200–300 nm in diameter and these small particles aggregated each other to form micro-sized spherical secondary particles. Hence, one can achieve both high rate capability and high tap density from the particles having the spherical morphology as shown in Fig. 2. Fig. 3 shows TEM images of the synthesized spherical $LiNi_{1/3}Co_{1/3}Mn_{1/3}O_2$ before and after coated with ZrO_2. Fig. 3a shows that the uncoated $LiNi_{1/3}Co_{1/3}Mn_{1/3}O_2$ has a smooth edge line without any layer on the surface. The newly formed coating layer on the surface of the ZrO_2-coated $LiNi_{1/3}Co_{1/3}Mn_{1/3}O_2$ particles is clearly seen in Fig. 3b. The thickness of the ZrO_2-coated layer on the surface of spherical $LiNi_{1/3}Co_{1/3}Mn_{1/3}O_2$ is estimated to be 10–25 nm in diameter. From the TEM images, it appears that ZrO_2 coating is rough and porous so we believe such a coating could reduce the direct contact between electrode and the electrolyte. Thus, it is reasonable to assume that the $LiNi_{1/3}Co_{1/3}Mn_{1/3}O_2$ surface coated with porous ZrO_2 coating layer would be suitable for Li^+ ion diffusion.

The electrochemical cycling performance was examined between 3.0 and 4.5 V at different C-rates at room temperature under same charge and discharge conditions. The cycling performances of the pristine and ZrO_2-coated $LiNi_{1/3}Co_{1/3}Mn_{1/3}O_2$ at different C-rates are presented in Fig. 4. The initial capacity of pristine material shows somewhat lower capacity than that of coated one at all the C-rates. On the other hand, pristine cathode material exhibits rapid capacity loss as the cycling rate increases, in agreement with the previous reports [27,28] whereas the capacity retention of the ZrO_2-coated cathode material was significantly improved at various C-rates. As shown in Fig. 4, the capacity of ZrO_2-coated material was 161 and 139 mAh g^{-1} at 0.1 and 1C-rates, respectively, after 40 cycles. These results suggest that the ZrO_2 coating on the spherical $LiNi_{1/3}Co_{1/3}Mn_{1/3}O_2$ is very effective in enhancing the electrochemical performance with respect to C-rate and capacity retention. In order to find whether the ZrO_2 coating still exists on the spherical $LiNi_{1/3}Co_{1/3}Mn_{1/3}O_2$ material, TEM measurements were carried out after several charge and discharge cycling. Fig. 5a and b show the TEM images of ZrO_2-coated spherical $LiNi_{1/3}Co_{1/3}Mn_{1/3}O_2$ after cycling at lower and higher magnifications, respectively. As seen in these figures, it is clear that the ZrO_2-coated $LiNi_{1/3}Co_{1/3}Mn_{1/3}O_2$ material still maintained its ZrO_2 coating, leading to relatively higher capacity retention as shown in Fig. 4. In general, all the electrochemical reactions take place on the surface of the electrodes for which the electrode must be in contact with electrolyte. Hence, according to the results obtained in this work, coating of ZrO_2 is effective in preventing direct contact of the active material with the electrolyte solution resulting in a decrease of electrolyte decomposition reactions. It is known that commercial $LiPF_6$-based lithium battery electrolytes always contain a trace amount of water. It has been established that the $LiPF_6$ can be reacted with traces of water and produce a very reactive HF species. Since ZrO_2 particle has a negative zeta potential and basic surface (pH > 7) [31] it can then scavenge and neutralize any unwanted acidic HF species present in electrolyte solution and thus preventing the active material from HF attack. ZrO_2 may also lower the activity of oxygen in providing strong Zr–O bonds at the active materials surface leading to an improved cycling stability of ZrO_2-coated active layered oxide materials [32].

In order to further understand the effect of the improvement of cycling behavior, the interrupt test was used to investigate the polarization effects in the charging and discharging process of each sample. Fig. 6 shows the potential gap between polarized potential and equilibrium potential of pristine and coated sample at charg-

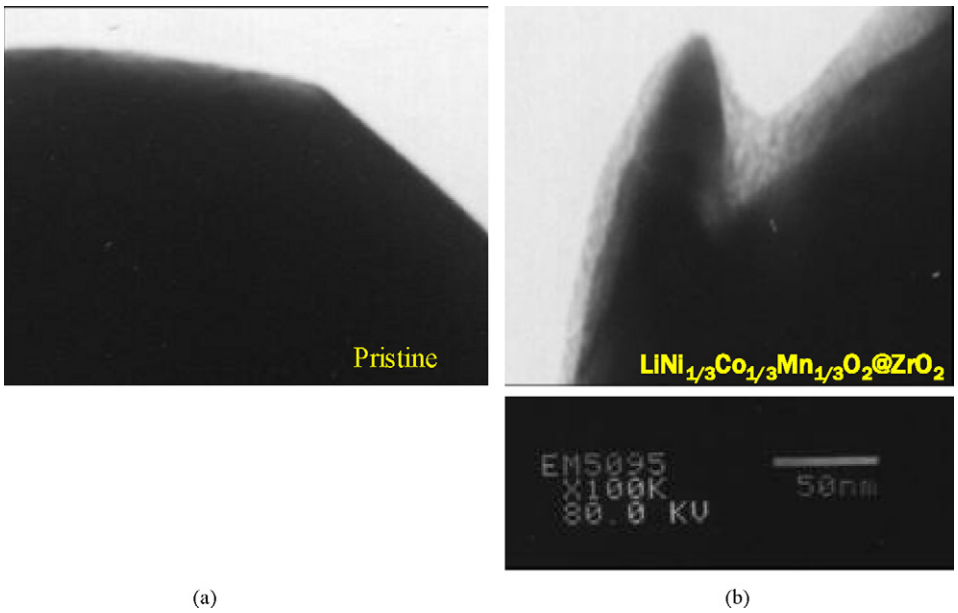

Fig. 3. TEM images of spherical (a) $LiNi_{1/3}Co_{1/3}Mn_{1/3}O_2$ and (b) ZrO_2-coated $LiNi_{1/3}Co_{1/3}Mn_{1/3}O_2$.

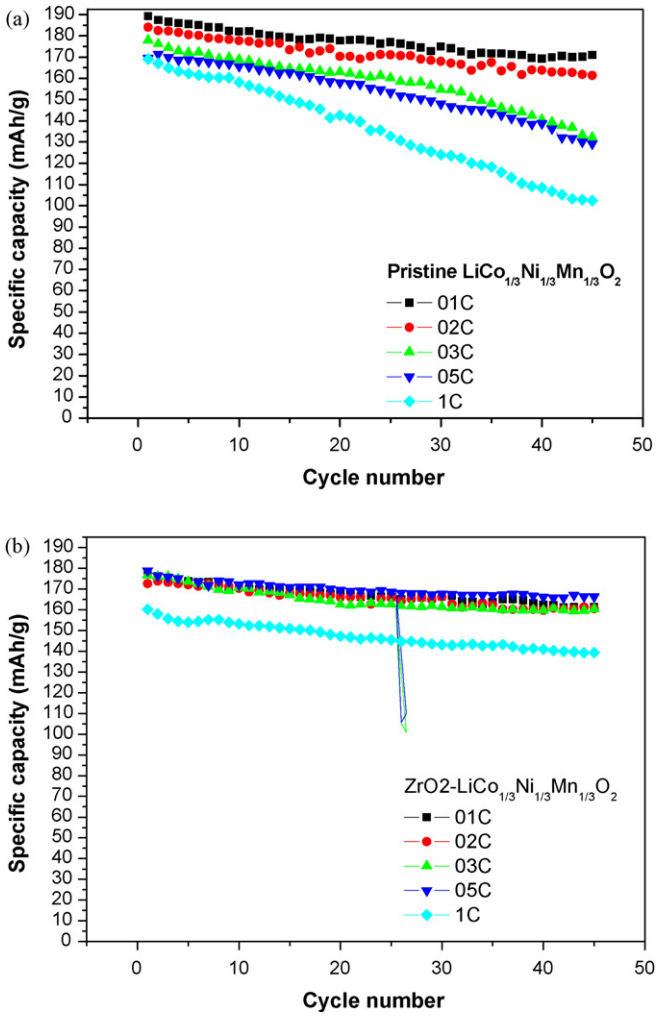

Fig. 4. Cycling performance of spherical (a) $LiNi_{1/3}Co_{1/3}Mn_{1/3}O_2$ and (b) ZrO_2-coated $LiNi_{1/3}Co_{1/3}Mn_{1/3}O_2$ at various C-rates between 3.0 and 4.5 V.

ing and discharging step. This potential gap might induce by both IR and the concentration of polarized Li^+ ions within the chosen time interval. The polarization of pristine $LiNi_{1/3}Co_{1/3}Mn_{1/3}O_2$ may be due to the extended reaction with the electrolyte and that can be the origin of the differences in the cell voltage during cell charge and discharge. As a result, the products of electrolyte degradation hinder fast lithium diffusion at the electrode–electrolyte interface. On the contrary, the polarization of ZrO_2-coated $LiNi_{1/3}Co_{1/3}Mn_{1/3}O_2$ is significantly reduced during charge and discharging process.

Impedance measurements were carried out at fully charged state (4.5 V) from 2nd cycle to 40th cycle for the pristine and ZrO_2-coated $LiNi_{1/3}Co_{1/3}Mn_{1/3}O_2$ to provide more information for the improved electrochemical performance. Since the polarization effect depends on the C-rate, the resistance of the cells made by pristine and ZrO_2-coated $LiNi_{1/3}Co_{1/3}Mn_{1/3}O_2$ materials was measured at various C-rates and the results are shown in Fig. 7a and b, respectively. As shown in this figure, one can see a great difference in cell resistance between pristine and coated material. The impedance of the pristine material increases drastically with cycle number at all the C-rates starting from 0.1C to 1C. Quantitatively, the impedance of the material at 2nd and 40th cycle at 0.2C was ~160 Ω and ~1100 Ω, respectively. However, the increase in the impedance of the ZrO_2-coated material is relatively very low from 2nd cycle to 40th cycle. The range of impedance variation for ZrO_2-coated material from 2nd cycle to 40th cycle is 70–210 Ω which is significantly lower than that of pristine material. The difference in the cell impedance between coated and uncoated material after 40 cycles is about 5 times. It is quite interesting to note that a thin coating of ZrO_2 on the active $LiNi_{1/3}Co_{1/3}Mn_{1/3}O_2$ material as shown in TEM image in Fig. 3b, obviously enhanced the kinetics of lithium intercalation and the conductivity of the coated material was not affected significantly even after cycling. This result shows that the improved electrochemical performances of ZrO_2-coated $LiNi_{1/3}Co_{1/3}Mn_{1/3}O_2$ material would be related with the lower impedance of coated active material which in turn is related with the thickness of the coating layer. From the results obtained from impedance measurements, it is clear that the diffusion coefficient of lithium ions is substantially improved by ZrO_2 coating on the active material during insertion and deinsertion reactions [29].

The thermal stability of the pristine and ZrO_2-coated $LiNi_{1/3}Co_{1/3}Mn_{1/3}O_2$ electrodes was measured at 4.5 V vs. Li

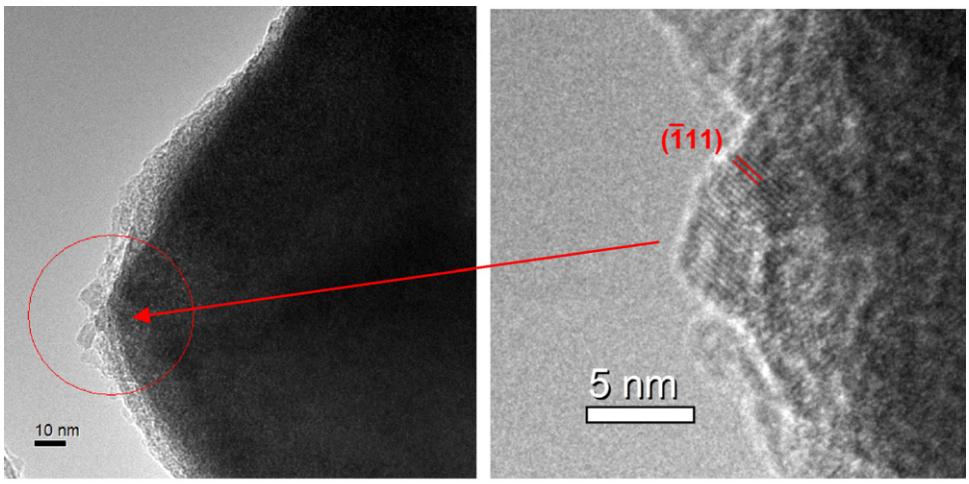

Fig. 5. TEM images of spherical ZrO_2-coated $LiNi_{1/3}Co_{1/3}Mn_{1/3}O_2$ after charge and discharge cycling: (a) lower magnification and (b) higher magnification.

using differential thermal calorimetry (DSC) and the DSC curves are shown in Fig. 8. It is seen that the on-set temperature ZrO_2-coated active material is close or a little lower than that of pristine. This might be due to the different state of charge between ZrO_2 coated and uncoated $LiNi_{1/3}Co_{1/3}Mn_{1/3}O_2$ material. Since ZrO_2-coated material shows lower impedance than pristine material (Fig. 7), more Li^+ ions are extracted from the ZrO_2-coated material, resulting in a little lower on-set temperature than pristine material. However, the heat amount associated with exothermic peak was reduced by ZrO_2 coating. The amount of heat generated for pristine and ZrO_2-coated $LiNi_{1/3}Co_{1/3}Mn_{1/3}O_2$ was 318.5 and 287.3 J g^{-1}, respectively. Even though a small amount of Zr is on the surface of the $LiNi_{1/3}Co_{1/3}Mn_{1/3}O_2$ electrode, it could introduce

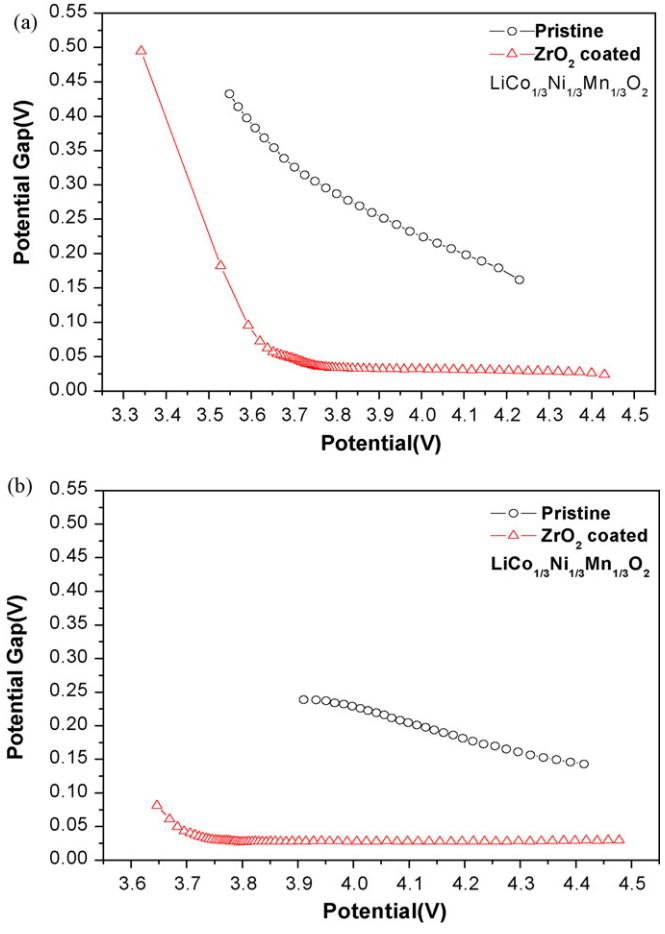

Fig. 6. The potential gap between polarized potential and equilibrium potential vs. potential of spherical $LiNi_{1/3}Co_{1/3}Mn_{1/3}O_2$ and ZrO_2-coated $LiNi_{1/3}Co_{1/3}Mn_{1/3}O_2$ during (a) charging process and (b) discharging process.

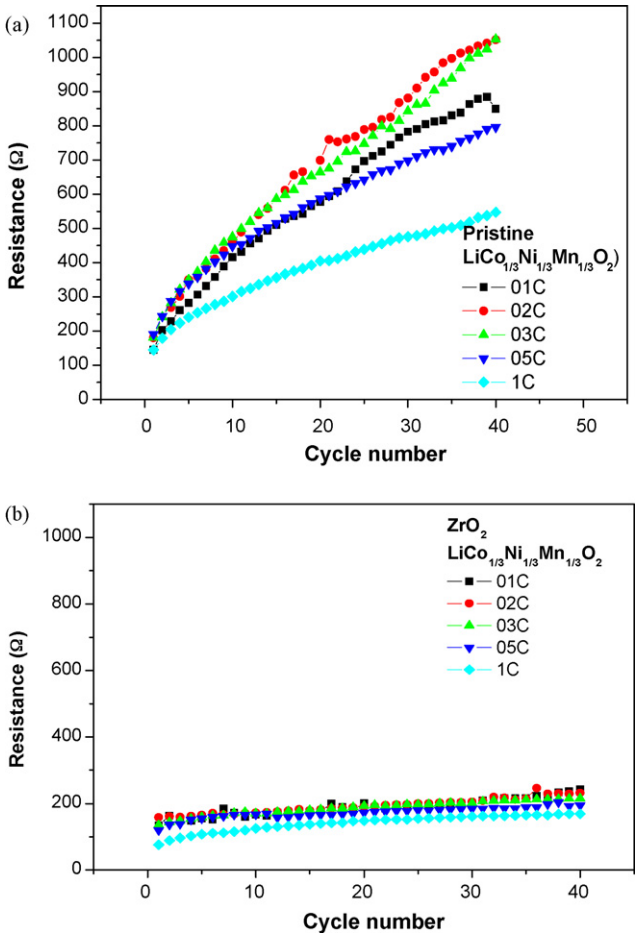

Fig. 7. Cell resistance vs. cycle for spherical (a) $LiNi_{1/3}Co_{1/3}Mn_{1/3}O_2$ and (b) ZrO_2-coated $LiNi_{1/3}Co_{1/3}Mn_{1/3}O_2$.

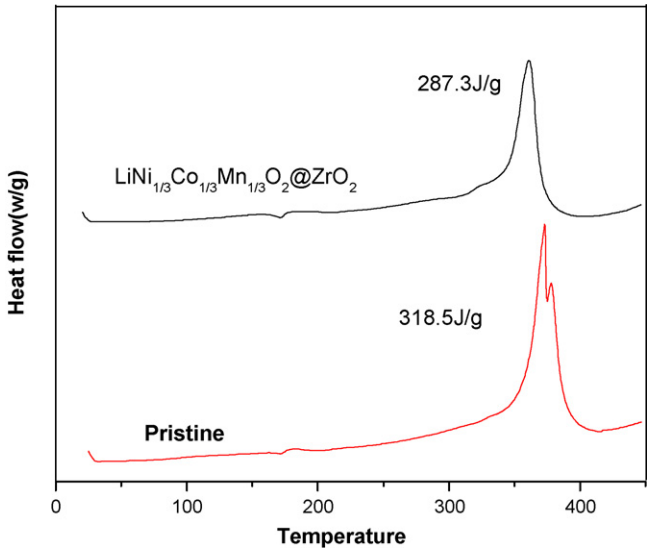

Fig. 8. DSC profiles of pristine and ZrO_2-coated $LiNi_{1/3}Co_{1/3}Mn_{1/3}O_2$ after charging to 4.5 V.

strong Zr–O bonds on the surface to lower the oxygen activity [32]. It is believed that this might be the possible reason why the amount of heat released from ZrO_2-coated electrode is lower than uncoated one. This result clearly suggests that the ZrO_2 coating on $LiNi_{1/3}Co_{1/3}Mn_{1/3}O_2$ protects the surface of the active material and suppresses the generation of oxygen significantly and thus improves the thermal stability.

The formation of the surface film is known to play a decisive role in the performance of the electrodes in Li ion cells. A mass deposition of the surface film on the electrode surface may end up as destructive film, which would decrease the electrode kinetics and hence its performance. The results of this work show that the deterioration in the electrochemical performance of the pristine $LiNi_{1/3}Co_{1/3}Mn_{1/3}O_2$ during repeated charge/discharge cycling is associated with the increase in resistance. The ZrO_2-coated $LiNi_{1/3}Co_{1/3}Mn_{1/3}O_2$ shows a lower cell resistance and excellent cycling performance when compared to pristine material and this may be due to the stable and minimal ZrO_2 surface film.

4. Conclusions

In this study, a ZrO_2-coated spherical $LiNi_{1/3}Co_{1/3}Mn_{1/3}O_2$ synthesized by a modified process, namely, co-precipitation method followed by spray drying process. Transmission electron microscopy analysis revealed that the thickness of the coated layer was 10–25 nm and was not diffused into the active materials. Electrochemical performances showed that the ZrO_2 coating was effective in improving the rate capability and cycling performance at a high cut-off voltage of 4.5 V. From the electrochemical impedance spectroscopy experiments, it was found that a significant improvement in the cycling stability was due to the suppression of impedance growth during charge and discharge cycling. From these results, the reason for the improved performance of ZrO_2-coated spherical $LiNi_{1/3}Co_{1/3}Mn_{1/3}O_2$ could be attributed to the ability of ZrO_2 to scavenge the HF species which is always present in trace amounts in the conventional lithium battery electrolytes. Thus, ZrO_2 coating protects the surface of the active material from HF attack and reduces the decomposition reactions significantly. Therefore, it can be concluded that a nano-sized ZrO_2 layer does not disturb the insertion and deinsertion reactions of lithium ionic species at the interface between active spherical $LiNi_{1/3}Co_{1/3}Mn_{1/3}O_2$ and the electrolyte and it significantly improves the cycling stability.

Acknowledgements

This research was financially supported by the National Science Council and National Taiwan University of Science and Technology (NTUST), Taiwan.

References

[1] H.K. Liu, G.X. Wang, Z. Guo, J. Wang, K. Konstantinov, J. Nanosci. Nanotechnol. 6 (2006) 1.
[2] M.S. Whittingham, Chem. Rev. 104 (2004) 4271.
[3] J.M. Tarascon, M. Armond, Nature 414 (2001) 359.
[4] Y. Kotama, Y. Makimura, I. Tanaka, H. Adachi, T. Ohzuku, J. Electrochem. Soc. 151 (2004) A1499.
[5] W.S. Yoon, Y. Paik, X.Q. Yang, M. Balasubramanian, J. McBreen, C.P. Grey, Electrochem. Solid-State Lett. 5 (2002) A263.
[6] T. Ohzuku, Y. Makimura, Chem. Lett. (2001) 642.
[7] B.J. Hwang, Y.W. Tsai, D. Cariler, G. Ceder, Chem. Mater. 15 (2003) 376.
[8] Y.W. Tsai, B.J. Hwang, G. Ceder, H.S. Sheu, D.G. Liu, J.F. Lee, Chem. Mater. 17 (2005) 3191.
[9] S.H. Park, C.S. Yoon, S.G. Kang, H.S. Kim, S.I. Moon, Y.K. Sun, Electrochim. Acta 49 (2004) 557.
[10] J. Cho, A. Manthiram, J. Electrochem. Soc. 152 (2005) A1714.
[11] S.W. Oh, S.H. Park, C.W. Park, Y.K. Sun, Solid State Ionics 171 (2004) 167.
[12] S. Jouanneau, K.W. Eberman, L.J. Krause, J.R. Dahn, J. Electrochem. Soc. 150 (2003) A1637.
[13] Y. Sun, C. Ouyang, Z. Wang, X. Huang, L. Chen, J. Electrochem. Soc. 151 (2004) A504.
[14] Y. Koyama, I. Tanaka, T. Ohuzuku, J. Power Sources 119–121 (2003) 644.
[15] M. Yoshio, H. Noguchi, J. Itoh, M. Okada, T. Mouri, J. Power Sources 90 (2000) 176.
[16] T.H. Cho, S.M. Park, M. Yoshio, T. Hirai, Y. Hideshima, J. Power Sources 142 (2005) 306.
[17] N. Yabuuchi, T. Ohuzuku, J. Power Sources 119–121 (2003) 171.
[18] J.M. Kim, H.T. Chung, Electrochim. Acta 49 (2004) 937.
[19] W. Yoon, C.P. Grey, M. Balasubramanian, X.Q. Yang, D.A. Fisher, J. McBreen, Electrochem. Solid-State Lett. 7 (2004) A53.
[20] W. Yoon, C.P. Grey, M. Balasubramanian, X.Q. Yang, Z. Fu, D.A. Fisher, J. McBreen, J. Electrochem. Soc. 151 (2004) A246.
[21] G.H. Kim, S.T. Myung, H.J. Bang, J. Prakash, Y.K. Sun, Electrochem. Solid-State Lett. 7 (12) (2004) A477.
[22] K.M. Shaju, G.V. Subba Rao, B.V.R. Chowadari, Electrochim. Acta 48 (2002) 145.
[23] K.M. Shaju, G.V. Subba Rao, B.V.R. Chowdari, J. Electrochem. Soc. 150 (2003) A1.
[24] Z. Chen, J.R. Dahn, Electrochem. Solid-State Lett. 5 (2002) A213.
[25] T. Ohzuku, A. Ueda, M. Nagayama, Y. Ieakoshi, H. Komori, Electrochim. Acta 38 (1993) 1159.
[26] Y. Gao, M.V. Yakovleva, W.B. Ebner, Electrochem. Solid-State Lett. 1 (1998) 117.
[27] J. Cho, G. Jim, H.S. Lim, J. Electrochem. Soc. 146 (1999) 3571.
[28] J. Cho, Y.J. Kim, B. Park, Chem. Mater. 12 (2000) 3788.
[29] J. Cho, Y.J. Kim, T.J. Kim, B. Park, Angew. Chem. Int. Ed. Engl. 40 (2001) 3367.
[30] K.M. Shaju, G.V. Subba, B.V.R. Chowdari, J. Electrochem. Soc. 151 (2004) A1324.
[31] Q. Xu, M.A. Anderson, J. Mater. Res. 6 (1991) 1073.
[32] M.M. Thackeray, C.S. Johnson, J.S. Kim, K.C. Lauzze, J.T. Vaughey, N. Dietz, D. Abraham, S.A. Hackney, W. Zeltner, M.A. Anderson, Electrochem. Commun. 5 (2003) 752.